THE EUROPEAN LARGE AREA ISO SURVEY: 90 MICRON NUMBER COUNTS

Philippe Héraudeau[1], Carlos del Burgo[1], Manfred Stickel[1], Andreas Efstathiou[2], Michael Rowan-Robinson[2], Csaba Kiss[3], Péter Ábrahám[3], Sebastian Oliver[4], Ulrich Klaas[1], and Dietrich Lemke[1]

[1] Max-Planck-Institut Für Astronomie, Königstuhl 17, Heidelberg, Germany

[2] Astrophysics Group, Blackett Laboratory, Imperial College, Prince Consort Rd, London SW7 2BW, UK

[3] Konkoly observatory of the Hungarian Acadamy of Sciences, P.O.Box 67, H-1525 Budapest, Hungary

[4] Astronomy Centre, CPES, University of Sussex, Falmer, Brighton BN1 9QJ , UK

ABSTRACT

The European Large Area ISO Survey (ELAIS) was the largest single Open Time project conducted by ISO, mapping an area of 12 square degrees at 15μm with ISOCAM and at 90μ with ISOPHOT. We first present the data analysis of the 90 μm survey. We show comparisons with model prediction for standard stars and with COBE/DIRBE for surface brightnesses of individual ELAIS fields and with the IRAS FSC catalog for 35 sources in common. The large number of rasters necessary to cover the wide ELAIS areas allows to compute a relative uncertainty for the calibration based on the FCS of typically 7%. From the comparison with standard stars model predictions, the absolute calibration is shown to be better than 15%.

The survey is 1.5 order of magnitude deeper than the IRAS 100μm survey and is expected to provide constraints on the formation and evolution of galaxies.

Finally, we present 90 μm number counts from a reliable subset of the detected sources. ELAIS number counts are compared to the evolutionary models of Guiderdoni (1998) and Rowan-Robinson (2001).

Key words: ISOPHOT; survey; galaxy evolution; Methods: data-analysis

1. OBSERVATIONS

The ELAIS survey was carried out in four main areas (three in the northern and one in the southern hemisphere) and some smaller areas of special scientific interest. The data consists of a number of P22 staring raster maps performed with the 3×3 array of the ISOPHOT instrument on-board ISO. The pixel size of the C100 detector is $43.5'' \times 43.5''$ on the sky and the C_90 filter with reference wavelength $90\mu m$ was used (see Oliver et al. 2000) for a complete description of the survey at 15,90 and $175\mu m$).

The area covered by each raster is typically 20×40 square arcminutes and the 4 largest fields are about 2.5 square degrees, N3 having the lowest coverage is only 2.1 square degree.

2. DATA PROCESSING

The data were first processed with PIA (PHT Interactive Analysis) version 9.1 using the OLP10 calibration files with however the improved dark signal and reset interval correction, and the consideration of by-passing sky light on the FCS (see Héraudeau et al. (2002a), del Burgo et al. (2002a) and del Burgo et al. (2002b) for details on ISOPHOT calibration).

The data reduction from ERD (Edited Raw Data) to SCP (Signal per Chopper Plateau) was performed using the so-called pairwise method developed by Manfred Stickel. The distribution of the difference between consecutive read-outs is used instead of making linear fits to the whole ramps. After rejecting the first 10% of the data stream which can be affected by transient, the mode of the distribution is estimated with myriad technique (Kalluri & Arce 1988) as the final signal for each raster position. This method has the advantage to be more robust against glitches caused by cosmic rays and which might create spurious sources in the data stream.

For each field, the relative uncertainty coming from the FCS calibration was computed as the mean absolute deviation of the average sky background of all rasters and is typically 7%.

3. SOURCE DETECTION AND CLASSIFICATION

The source detection was performed using the Sextractor software, version 2.2.2 (Bertin & Arnouts 1996), on the final map. To ensure the reliability of the sources detected by Sextractor, we confront them to eye-balled classification based on the time sequence analysis of the data streams (See Surace et al. 1999). For each source detected by Sextractor we look for the classifications of detections around the central position within the size of the C100 detector array. We retain sources which were classified at least twice as a source and with a signal-to-noise ratio larger then 3.

4. CALIBRATION

4.1. STANDARD STARS

In order to better determine the ELAIS calibration (as well as the general ISOPHOT calibration) three stars (HR6132, HR6464 and HR5981) close to the ELAIS fields were observed in mini-raster mode (a 3×3 raster with the star positioned at the centre of a different pixel in each pointing). The faintest of the stars (HR598) was observed twice on the same ISO orbit. To increase the sample of measurements and thus the reliability of the comparison we selected all other standard stars from the archive also observed in mini-raster mode at $90\mu m$. These stars also formed part of the ISO ground based preparatory programme. Models for their far-IR spectra were constructed by

Proceedings of the Symposium *"Exploiting the ISO Data Archive - Infrared Astronomy in the Internet Age"*, 24–27 June 2002, Sigüenza, Spain (C. Gry, S. B. Peschke, J. Matagne et al. eds., ESA SP-511)

fitting near-IR data and extrapolating to longer wavelengths as ν^2 (Hammersley et al. 1998). A more empirical approach was given by Cohen et al. (1999). The predicted stellar fluxes lie in the range 0.06 - 10Jy. Tab. 1 shows the list of stars and the characteristics of the measurements as well as predicted fluxes. The integration time per pointing in these mini-rasters (from 40 to 72s) is longer than that used for the bulk of the ELAIS survey in order to obtain an accurate determination of fluxes to establish the ISOPHOT calibration. The observations of calibration stars were processed in the same way as the survey rasters. Results of the comparison are given in Tab. 1 as the ratio between measured (based on the FCS) and theoretical fluxes. When two model predictions were available, we used their mean to compute the ratio. The two measurements on *HR5981* are in agreement within 5%. ISOPHOT fluxes are systematically higher than the predicted ones and the mean ratio is 1.12 ± 0.11.

4.2. Comparison to COBE/DIRBE

The extensions of the large ELAIS fields make them appropriate for a comparison of their sky background brightnesses with COBE/DIRBE without being hampered by the lower resolution of the latter. For a systematic comparison of ISOPHOT versus DIRBE surface brightnesses see Héraudeau et al. (2002a).

Fig. 1 shows the comparison of DIRBE versus ISOPHOT surface brightnesses. Error bars for DIRBE are typically equal to $0.06 MJy/sr$. Error bars for Phot come from the rms of the rasters sky background level for each series of measurement and are typically $0.2 MJy/sr$.

The relationship is well fitted with a straight light of the form:

$$\mathrm{SB(ISOPHOT)} = 0.55 \pm 0.56 + 1.30 \pm 0.16 \times \mathrm{SB(DIRBE)}$$

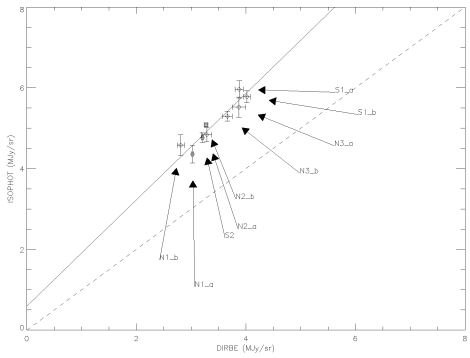

Figure 1. Comparison of ISO and COBE/DIRBE surface brightnesses for the ELAIS fields. The largest fields (N1,N2,N3 and S1 are divided into two sets of measurements ($N1_a, N1_b$, etc...) which were performed at different period of the year and therefore may have different Zodiacal light contribution. DIRBE values were interpolated at $90\mu m$. The solid line is the result of fitting the points with a straight line. The dotted line represents a slope of unity.

4.3. Comparison with *IRAS* sources

While the ELAIS fields were chosen to avoid strong infrared sources, there are a number of IRAS $100\mu m$ sources in the PSC and FSC which were detected in the survey. The fluxes of these 35 sources lie in the range $0.2Jy \leq S(100) \leq 2.1Jy$. Fig. 2 shows the comparison with the FSC catalogue which is the more accurate at this faint level. All common sources have low (the flux is an upper limit) or intermediate IRAS quality flags. Color correction factors were computing from the IRAS 4-band Spectral Energy Distribution and IRAS and ISOPHOT filter profiles.

Optical identifications of these sources appear to be galaxy pairs or galaxies. Three of them are stars. The mean difference between IRAS and ISOPHOT is 0.086 Jy and the standard deviation is 0.20 Jy for IRAS data with intermediate quality flag (2) only.

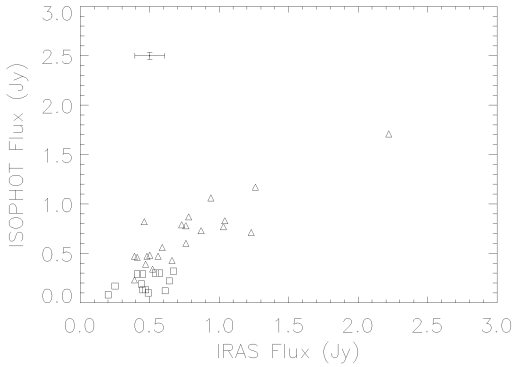

Figure 2. Comparison of ISOPHOT and IRAS/FSC fluxes at 90 micron for 35 common sources in the ELAIS fields. The $90\mu m$ fluxes of the IRAS sources are estimated by linearly interpolating between the color-corrected 60 and $100\mu m$ fluxes. Squares and triangles correspond to IRAS sources with quality flag equal to 1 (upper limit) and 2 (intermediate quality). Typical error bars are indicated in the upper-left part of the diagram.

4.4. Conclusion on calibration

We rescaled our photometry according to the difference found for standard stars (i.e. a factor 1.12). This correction also goes towards the same direction than the slope of the relationship found for surface brightnesses between ISO and DIRBE which is somewhat larger (a factor 1.30). As we are mainly interested in calibrating point sources we do not use the scaling factor coming from the surface brightnesses comparison which may involve additional uncertainties coming from the determination of solid angles.

5. NUMBER COUNTS

The resulting integral counts are given in Fig. 3 (points) where are also plotted the IRAS counts (see Efstathiou et al. 2001).

Table 1. The list of standard stars used to check the FCS calibration with theoretical values. TDT numbers of measurements, name of stars, exposure time, size of the mini-rasters, model predictions from M. Cohen ('MC') and P. Hammersley ('PH') as well as ISOPHOT fluxes and their uncertainties are indicated. "Ratio" is the ratio between measured and predicted fluxes. When two model predictions were available, we used their mean to compute the ratio. "Iras" is the IRAS flux extrapolated from the 60μm flux when the quality flag was good.

Measurement	Name	Exposure	RI	Size	$F(MC)$	$F(PH)$	Pht	e_pht	Ratio	Iras
		sec	sec		Jy	Jy	Jy	Jy	–	Jy
08602417	HR5340	37.00	0.12	5	9.308	9.029	9.589	0.360	1.046	8.573
10503417	HR6705	72.00	0.50	5	2.013	1.904	2.424	0.139	1.237	2.001
27502117	HR5340	72.00	0.25	5	9.308	9.029	9.593	0.233	1.046	8.573
29301005	HR7310	72.00	4.00	5	0.258	0.268	0.330	0.022	1.281	0.251
39103002	HR8775	72.00	0.25	5	4.961	5.096	5.777	0.143	1.149	5.300
65701318	HR1654	72.00	1.00	3	0.713	–	0.744	0.026	1.044	0.666
72701418	HR7980	72.00	1.00	3	0.517	–	0.477	0.024	0.923	0.488
77200361	HR5981	40.00	2.00	3	–	0.063	0.071	0.015	1.131	–
77200364	HR5981	40.00	2.00	3	–	0.063	0.066	0.010	1.058	–
78300465	HR6464	40.00	2.00	3	–	0.120	0.157	0.020	1.310	–
78300677	HR6132	40.00	2.00	3	–	0.288	0.323	0.023	1.121	–
63801807	HR7451	54.00	1.00	3	–	0.0075	0.0427	0.010	5.696	–

ELAIS counts are corrected for incompleteness estimated from the number of recovered simulated sources on the maps.

5.1. Comparison with evolutionary models

In figure 3 we also compare the observed counts with the evolutionary models of Rowan-Robinson (1999) and Guiderdoni et al. (1998).

The model of Rowan-Robinson includes four spectral components: infrared cirrus (emission from interstellar dust), an M82-like starburst, an Arp220-like starburst and an AGN dust torus.

The model of Guiderdoni et al. is set within the framework of hierarchical growth of structures according to the cold dark matter model, and extends earlier studies to the IR/submm wavelength regime. In Fig. 3 we plot the prediction from their models A and E. The latter model incorporates a heavily extinguished (ULIRG) population, assumed to dominate at high redshift in order to account for the far-ir background.

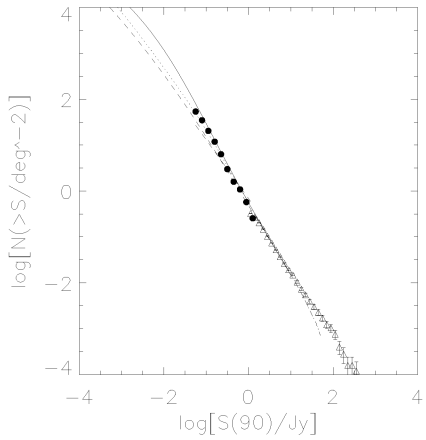

Figure 3. ELAIS 90μm number counts. The solid line represents the model of Rowan-Robinson (1999), the dashed and dotted lines show model A et E respectively of Guiderdoni et al. (1998). Iras number counts are also plotted (triangles).

6. Summary and conclusion

We have re-analysed ELAIS 90μm data with the so-called "pairwise" method which is more robust against glitches than the usual ramp fitting. We selected sources with a signal-to-noise ratio larger than 3 and which were classified as a real source by at least 2 people to ensure their reliability.

The ELAIS counts extend the IRAS counts by 1.5 order of magnitude in flux. The slope of the counts is consistent with the strong evolution seen in other infrared and submillimeter surveys.

Within the uncertainties associated with the flux calibration of the survey, the counts agree with the strongly evolving models of Rowan-Robinson (1999) and Guiderdoni et al. (1998) favouring the model E of the latter.

Acknowledgements

ELAIS was supported by EU TMR Network FMRX-CT96-0068 and PPARC grant GR/K98728.

Carlos del Burgo acknowledges support from the EC TMR Network POE.

The development and operation of ISOPHOT were supported by MPIA and funds from Deutsches Zentrum für Luft- und Raumfarht (DLR, formerly DARA). The ISOPHOT Data Center at MPIA is supported by Deutsches Zentrum für Luft- und Raumfarht e.V. (DLR) with funds of Bundesministerium für Bildung und Forschung, grant No. 50 QI 9801 3. The authors are responsible for the contents of this publication.

REFERENCES

Del Burgo, C., Ábrahám, P., Klass, U. and Héraudeau., P., 2002a, ESA SP-428 , in press.

Del Burgo, C., 2002b, this volume.

Efstathiou, A. et al., MNRAS, 2000, Vol 319,4, p. 1169-1177.

Guiderdoni, B., Hivon, E., Bouchet, F.R., Maffei, B., MNRAS, 1998, 295, 877.

Héraudeau, Ph., Ábrahám, P., Klaas, U., Kiss, C., 2002a, ESA, SP-428, in press

Héraudeau, Ph. Ábrahám, P., Klaas, U., Del Burgo , C. , 2002b, ESA SP-428, in press.

Kalluri, S. and Arce, G.R., 1998, IEEE Transactions on Signal Processing 46 ,322.

Rowan-Robinson, M. , 2001, Lecture Notes in Physics, vol. 548, p.129.

Oliver, S. and ELAIS consortium, MNRAS, 2000, Vol. 316,4, p. 749-767.

Surace, C., Héraudeau, Ph., U., Lemke, D., Oliver, S., Rowan-Robinson ELAIS, ISOPHOT results, 1999, ESA SP-427,Vol. 2, p. 1059-1062.

TECHNICAL CONTRIBUTIONS